CANCER

Afatinib restrains K-RAS–driven lung tumorigenesis

Herwig P. Moll[1], Klemens Pranz[2], Monica Musteanu[3], Beatrice Grabner[2],
Natascha Hruschka[2], Julian Mohrherr[2], Petra Aigner[2], Patricia Stiedl[2], Luka Brcic[4],
Viktoria Laszlo[5,6], Daniel Schramek[7,8,9], Richard Moriggl[2,10,11], Robert Eferl[12], Judit Moldvay[13],
Katalin Dezso[14], Pedro P. Lopez-Casas[3], Dagmar Stoiber[2,15], Manuel Hidalgo[3],
Josef Penninger[7], Maria Sibilia[12], Balázs Győrffy[16], Mariano Barbacid[3], Balázs Dome[5,6,13,17],
Helmut Popper[4], Emilio Casanova[1,2]*

On the basis of clinical trials using first-generation epidermal growth factor receptor (EGFR) tyrosine kinase inhibitors (TKIs), it became a doctrine that V-Ki-ras2 Kirsten rat sarcoma viral oncogene homolog (K-RAS) mutations drive resistance to EGFR inhibition in non–small cell lung cancer (NSCLC). Conversely, we provide evidence that EGFR signaling is engaged in K-RAS–driven lung tumorigenesis in humans and in mice. Specifically, genetic mouse models revealed that deletion of Egfr quenches mutant K-RAS activity and transiently reduces tumor growth. However, EGFR inhibition initiates a rapid resistance mechanism involving non-EGFR ERBB family members. This tumor escape mechanism clarifies the disappointing outcome of first-generation TKIs and suggests high therapeutic potential of pan-ERBB inhibitors. On the basis of various experimental models including genetically engineered mouse models, patient-derived and cell line–derived xenografts, and in vitro experiments, we demonstrate that the U.S. Food and Drug Administration–approved pan-ERBB inhibitor afatinib effectively impairs K-RAS–driven lung tumorigenesis. Our data support reconsidering the use of pan-ERBB inhibition in clinical trials to treat K-RAS–mutated NSCLC.

INTRODUCTION

Lung cancer is still the number one cancer-related killer in men and women, with less than 20% of patients surviving more than 5 years (1). Lung adenocarcinomas (ACs), the most common non–small cell lung cancer (NSCLC) subtype, are stratified by different driver mutations, with activating mutations in K-RAS and EGFR being the most abundant ones (2, 3). Although treatment with epidermal growth factor receptor (EGFR)–targeting small-molecule tyrosine kinase inhibitors (TKIs) such as erlotinib, gefitinib, or afatinib is initially effective in lung cancer patients with common activating EGFR mutations, acquisition of resistance almost inevitably occurs (4–7). In contrast and despite extensive research, there is no effective inhibitor targeting mutated K-RAS protein available in the clinics (8). Traditionally, oncogenic K-RAS mutations were thought to render the protein consti-

tutively active and independent from its upstream activator EGFR (9). Therefore, K-RAS mutations have been proposed as a mechanism of primary resistance to EGFR TKI, and many studies demonstrated poor clinical outcomes using erlotinib and gefitinib in patients with NSCLC harboring K-RAS mutations (10–13). In contrast, more recent work demonstrated that mutated K-RAS is not completely locked in its active form. The combination of an irreversible inhibitor specific to K-RAS[G12C] together with erlotinib or gefitinib in K-RAS[G12C]–mutated lung cancer cell lines showed synergistic effects, demonstrating that mutated K-RAS is activated by upstream EGFR (14, 15). Our finding that K-RAS–driven lung ACs display increased expression of EGFR and its ligands, as well as downstream targets, supports this discovery and prompted us to clarify whether EGFR signaling contributes to the development of this disease.

RESULTS

ERBB signaling is activated in human K-RAS–mutated lung AC

We analyzed publicly available mRNA expression data (GSE75037) by transcriptional profiling and hierarchical clustering of human K-RAS–mutated tumor biopsies versus adjacent nontumorous lung tissue using gene signatures of ERBB activation. K-RAS–driven lung AC tissue showed a uniform expression pattern of genes involved in ERBB signal transduction (Fig. 1A and fig. S1A) (16), and mRNA expression of these genes in the tumor tissue was enriched as compared to nonmalignant tissue (Fig. 1B) (17). Furthermore, gene ratios of K-RAS–mutated tumor versus adjacent lung parenchyma in patients suffering from stage II and higher lung AC indicate an impact of ERBB signaling during malignant progression (Fig. 1C). In particular, we observed mRNA up-regulation of the ERBB family receptors and several of its ligands in human K-RAS–mutated lung AC tissue compared to adjacent parenchyma (Fig. 1D). Although an increased K-RAS gene signature and the expression of genes associated with poor survival in the tumors versus nonmalignant tissue validated the gene set

[1]Department of Physiology, Center of Physiology and Pharmacology and Comprehensive Cancer Center (CCC), Medical University of Vienna, AT-1090 Vienna, Austria. [2]Ludwig Boltzmann Institute for Cancer Research, AT-1090 Vienna, Austria. [3]Spanish National Cancer Research Centre, E-28029 Madrid, Spain. [4]Institute of Pathology, Medical University of Graz, AT-8036 Graz, Austria. [5]Division of Thoracic Surgery, Department of Surgery and CCC, Medical University of Vienna, AT-1090 Vienna, Austria. [6]Department of Biomedical Imaging and Image-guided Therapy, Division of Molecular and Gender Imaging, Medical University of Vienna, AT-1090 Vienna, Austria. [7]Institute of Molecular Biotechnology of the Austrian Academy of Sciences, AT-1030 Vienna, Austria. [8]Center for Systems Biology, Lunenfeld-Tanenbaum Research Institute, Mount Sinai Hospital, ON-M5G 1X5 Toronto, Ontario, Canada. [9]Department of Molecular Genetics, University of Toronto, ON-M5S 1A8 Toronto, Ontario, Canada. [10]Institute of Animal Breeding and Genetics, University of Veterinary Medicine Vienna, Medical University of Vienna, AT-1210 Vienna, Austria. [11]Medical University of Vienna, AT-1090 Vienna, Austria. [12]Institute of Cancer Research, Medical University of Vienna and CCC, AT-1090 Vienna, Austria. [13]Department of Tumor Biology, National Korányi Institute of Pulmonology, Semmelweis University, HU-1122 Budapest, Hungary. [14]First Department of Pathology and Experimental Cancer Research, Semmelweis University, HU-1122 Budapest, Hungary. [15]Institute of Pharmacology, Center for Physiology and Pharmacology, Medical University of Vienna, AT-1090 Vienna, Austria. [16]MTA TK Lendület Cancer Biomarker Research Group, Institute of Enzymology and Second Department of Pediatrics, Semmelweis University, HU-1122 Budapest, Hungary. [17]Department of Thoracic Surgery, National Institute of Oncology and Semmelweis University, HU-1122 Budapest, Hungary.
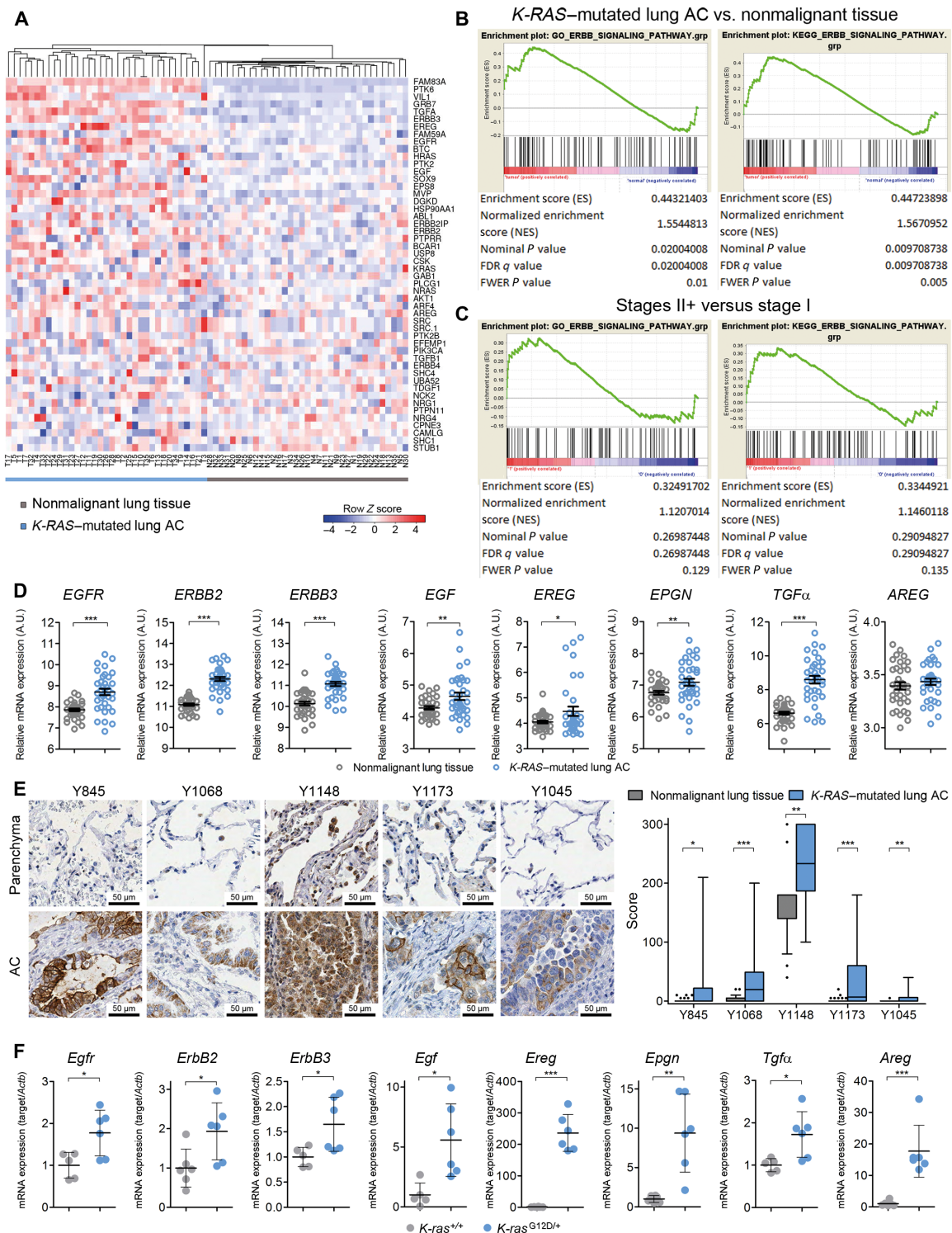*Corresponding author. Email: emilio.casanova@meduniwien.ac.at

Fig. 1. K-RAS–mutated lung ACs display increased EGFR activity. (**A**) Heat map for mRNA expression in K-RAS–mutated tumor biopsies (T1 to T35) and adjacent nonmalignant, healthy lung parenchyma (N1 to N35) of the same patients. Displayed are the top 50 differentially regulated genes within the Gene Ontology (GO) ERBB signaling pathway (GO: 0038127). Hierarchical clustering was performed using heatmapper.ca online tool. (**B**) GSEA for GO and KEGG ERBB pathway signatures in K-RAS–mutant tumors versus nonmalignant tissue and (**C**) in K-RAS–mutated tumors of stage II and higher versus stage I. FDR, false discovery rate; FWER, familywise-error rate. (**D**) Relative mRNA expression of indicated genes in healthy lung tissue and K-RAS tumors. $n = 35$ per group, data shown as means ± SD. Data in (A) to (D) were retrieved from the Gene Expression Omnibus (GSE75037). A.U., arbitrary units. (**E**) Images of representative immunohistochemical staining for indicated EGFR phosphorylation sites in human nonmalignant lung parenchyma and K-RAS–mutated lung AC. Boxplot (min to max) of scoring values shows EGFR phosphorylation specifically in tumor cells versus healthy tissue. $n \geq 30$ per group. (**F**) Relative mRNA expression in WT (K-ras^{+/+}, $n = 5$ to 6) and tumor-bearing mouse lungs (K-ras[G12D/+], $n = 6$) at 10 weeks after tumor induction via Ad.Cre treatment. Actb was used for normalization. Data are presented as means ± SD. (D to F) *$P < 0.05$, **$P < 0.01$, ***$P < 0.001$.

used (fig. S1B), the analysis of bulk tumor samples does not allow to discriminate whether the observed activation of ERBB signaling stems from tumor cells or the stroma. Hence, we performed immunohistochemistry on resected samples of *K-RAS*–mutated mucinous human lung AC and paired nontumorous lung parenchyma, probing for the activating tyrosine phosphorylation sites Y845, Y1068, Y1148, and Y1173 and inactivating site Y1045 (Fig. 1E and fig. S2A). Analysis of the sections by board-certified pathologists revealed positive tumor cells for all phosphorylation sites, whereas staining for Y1068 and Y1173 was completely absent in the stromal compartment, and staining intensity of Y1148 was much stronger in tumor cells compared to the stroma. Phosphorylation of Y1045, which counteracts EGFR activation (*18*), was restricted to tumor cells and endothelial cells but absent on most tumor samples. Grading of phospho-EGFR expression demonstrated enhanced activation of EGFR in tumor cells as compared to healthy lung parenchyma (Fig. 1E). Moreover, we did not observe significant differences in the activation of EGFR in tumor cells from wild-type (WT) K-RAS or mutated EGFR tumors, indicating that EGFR is activated in lung AC independently of the oncogenic driver (fig. S2B). We then took advantage of a second cohort of patients harboring *K-RAS*–mutated lung AC and confirmed expression of EGFR and its activation, as marked by an additional activating phosphorylation site at Y1086 in tumor cells (fig. S2C). In addition, we found that ERBB2 was expressed and activated in those tumors (fig. S2, C and D). Because mucinous lung AC often lack the transcription factor NK2 homebox 1 (NKX2-1), we checked NKX2-1 expression in the human lung AC samples and found that tumors from both cohorts showed heterogeneous NKX2-1 expression (fig. S2, E and F). Together, these data demonstrate that ERBB signaling is activated in human K-RAS–driven lung AC in tumor cells and, to some extent, in stromal cells.

Genetic EGFR ablation impairs growth of *K-RAS*–mutated lung AC

Next, we analyzed the mRNA expression profile of tumor-bearing lungs derived from a mouse model of autochthonous lung tumors driven by oncogenic *K-ras* (*19, 20*). In line with the data for human lung AC, we observed increased expression of several members of the EGFR-ERBB signaling pathway upon *K-ras*^{G12D}–driven lung tumorigenesis, indicating a key role of EGFR-mediated signaling in this genetically engineered mouse model (GEMM; Fig. 1F).

To test the impact of EGFR-mediated signal transduction in K-RAS–driven lung tumorigenesis, we crossed *K-ras*$^{LSL-G12D}$ (K) mice (*19*) with *Egfr* floxed/floxed (*21*) mice. Inhalation with Ad.Cre allowed for concomitant *K-ras*^{G12D} activation and *Egfr* deletion in developing lung tumors in the *K-ras*^{G12D}:*Egfr*$^{ΔLep/ΔLep}$ (KE) mice and resulted in significantly (*P* < 0.0001) prolonged survival of mice as compared to K mice (Fig. 2A). Similarly, in mice with *K-ras*^{G12D} activation and simultaneous deletion of *p53* (*22*) in lung epithelial cells (*K-ras*^{G12D}:*p53*$^{ΔLep/ΔLep}$, hereafter KP), a GEMM representing advanced lung ACs (*23*), we also observed a survival benefit when *Egfr* was deleted in K-ras^{G12D}:p53$^{ΔLep/ΔLep}$:Egfr$^{ΔLep/ΔLep}$ (KPE) mice (Fig. 2B). This survival effect was dose-dependent, and mice harboring tumors with heterozygous deletion of *Egfr* also exhibited advanced survival times compared to K and KP mice but decreased survival compared to KE mice (Fig. 2, A and B). To confirm efficient and complete recombination of the floxed *Egfr* allele in the developing tumor cells, we isolated tumor cells from the lungs of KP and KPE mice used in the survival analysis after death of the animals. Genotyping of these

KP and KPE cells after passaging them 5 to 10 times in vitro ruled out incomplete recombination of *Egfr* (fig. S3A).

In these models, stromal and epithelial cells have the potential to be transduced by Ad.Cre, resulting in recombination of transgenes within these cells and eventually triggering S100-positive Langerhans cell histiocytosis-like neoplasms (*24, 25*). Although most tumor cells stained positive for the alveolar type II (AT2) marker surfactant protein C (SP-C, fig. S3B), whereas S100 expression was restricted to single stromal cells, we cannot exclude that *Egfr* deletion in stromal cells might contribute to the observed phenotype. Therefore, we performed orthotopic transplantation of KP and KPE tumor cells isolated from the lungs of KP and KPE mice at 6 weeks after Ad.Cre inhalation. As in the Ad.Cre model, mice harboring EGFR-deficient *K-ras*–mutated transplanted tumors exhibited a survival advantage compared to mice injected with EGFR-expressing *K-ras*–mutated lung AC cells, further demonstrating that tumor cell–intrinsic deletion of *Egfr* impairs growth of *K-ras*–mutated lung AC (Fig. 2C).

For histopathologic analysis, we first verified EGFR knockout in lung tumor sections of KE mice 10 weeks after Ad.Cre inhalation (fig. S3C). Mice harboring *Egfr* knockout tumors exhibited reduced tumor burden, which was also reflected by reduced lung–to–body weight ratios (Fig. 2D and fig. S3D). Furthermore, the increase in *Sp-c* mRNA expression in lungs of K mice compared to healthy lungs reflects a higher abundance of AT2 cells, the main cell type of origin of K-RAS–driven lung AC, which was reduced in KE mice (fig. S3E) (*26–28*). There was no difference in the number of total tumors per area or tumor grade in KE as compared to K mice (Fig. 2D and fig. S3F). KE mice showed reduced tumor cell proliferation but no difference in apoptosis when compared to K mice (Fig. 2E and fig. S3G). Downstream of K-RAS signaling, we found decreased activation of extracellular signal–regulated kinase 1 and 2 (ERK1/2) in tumors of KE mice (Fig. 2E). However, activation of serine-threonine protein kinase Akt was higher in the KE group, most likely to compensate for the loss of EGFR (fig. S3H). At the mRNA level, loss of *Egfr* also reduced mRNA expression of EGFR ligands in mouse lungs 10 weeks after tumor induction (fig. S3I).

Next, we used CRISPR-Cas9 technology to generate *EGFR*-deficient isogeneic clones of the human lung AC cell line A549, which harbors a homozygous *K-RAS*^{G12S} mutation, with and without concomitant *p53* deletion (fig. S4A). *EGFR* deficiency reduced in vitro growth of A549 cells (Fig. 2F and fig. S4B). Furthermore, *EGFR* deficiency interfered with A549 tumor growth after xenotransplantation into immunodeficient nonobese diabetic severe combined immunodeficient gamma (NSG) mice, regardless of the *p53* status (Fig. 2G and fig. S4C). Together, these data demonstrate that growth of *K-RAS*–mutated lung AC depends on upstream expression of EGFR both in vitro and in vivo.

Mutant K-RAS activity in lung AC depends on upstream EGFR activation

Next, we aimed to identify the key signaling nodes affected by the loss of EGFR in *K-RAS*–mutated lung AC cells. Therefore, we isolated primary mouse alveolar type 2 pneumocytes from the lungs of WT, K, and K-*Egfr* floxed/floxed mice and transduced cells in vitro with Ad.Cre. We confirmed purity of cell isolates, activation of mutated *K-ras*, and loss of *Egfr* in K and KE cells 2 days after transduction (fig. S5, A and B). Five days after Ad.Cre treatment, we retrieved RNA of WT, K, and KE cells and subjected it to RNA sequencing (RNA-seq) analysis. As in bulk tumor tissue of human and mouse origin, we detected a significant (*P* < 0.0001) increase in *Egfr* expression in primary cell
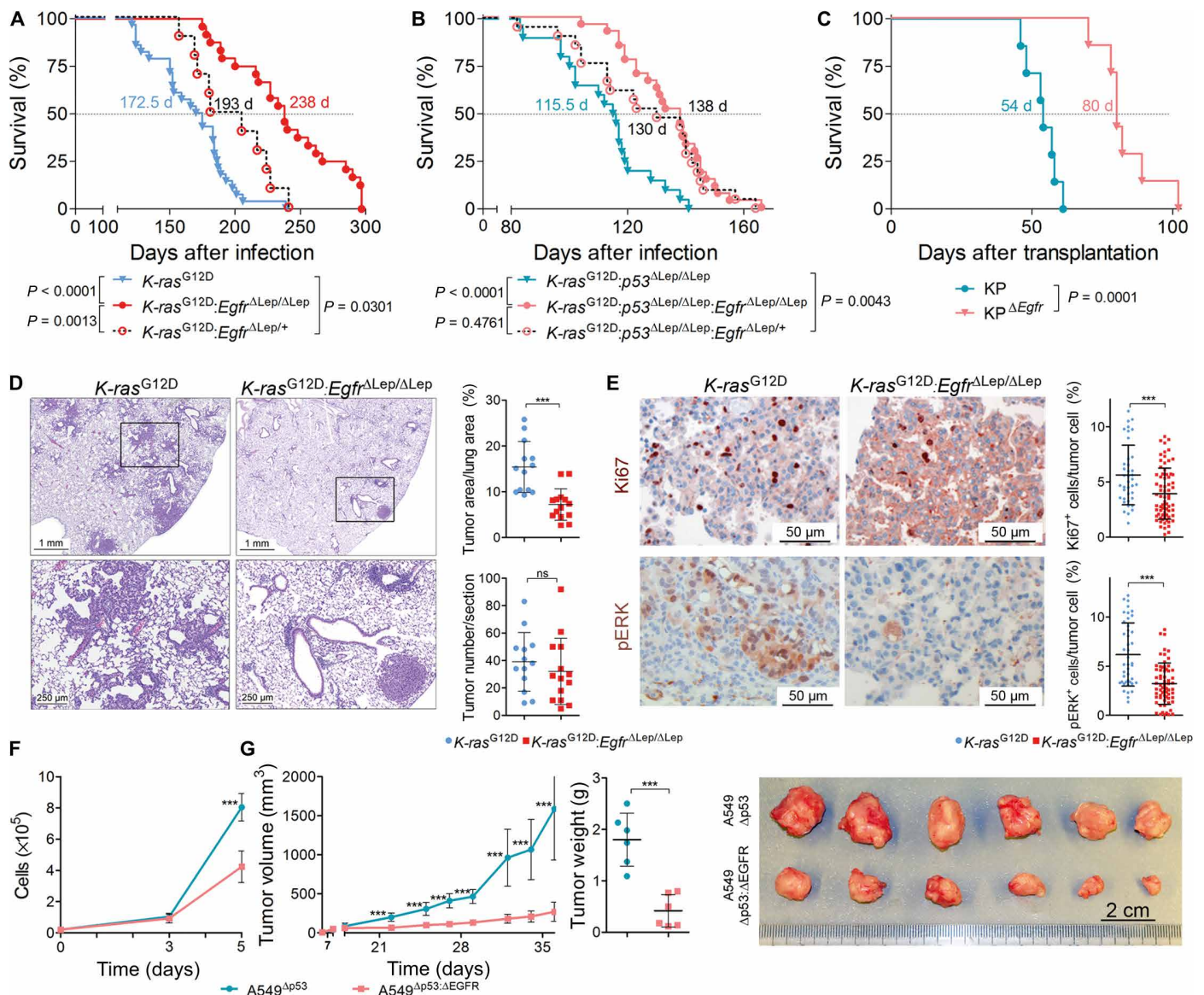
Fig. 2. Genetic EGFR ablation in *K-RAS*–mutated lung AC reduces tumor growth. (**A**) Kaplan-Meier analysis of K (*K-ras*^G12D, *n* = 24) and KE (*K-ras*^G12D:*Egfr*^ΔLep/ΔLep, *n* = 28) mice and (**B**) of KP (*K-ras*^G12D:*p53*^ΔLep/ΔLep, *n* = 20) and KPE (*K-ras*^G12D:*p53*^ΔLep/ΔLep:*Egfr*^ΔLep/ΔLep, *n* = 27) mice after intranasal infection with Ad.Cre. (**C**) Survival analysis of immunocompetent recipient mice after orthotopic transplantation of syngeneic *K-ras*^G12D–mutated and p53-deficient KP cells, with and without *Egfr* deletion (*n* = 7 per group). (A to C) The median survival times of the groups are indicated. Differences in survival of groups were tested for significance using the log-rank test, and respective *P* values are shown. (**D**) Representative images of hematoxylin and eosin (H&E) staining, including higher magnification of the indicated areas (bottom) of tumor-bearing lungs 10 weeks after Ad.Cre inhalation of mice with specified genotypes. For quantitation, the mean values of two sections per mouse were used. Graphs represent means of ratios ± SD of tumor area versus healthy lung area and mean tumor numbers ± SD per section (*n* = 13 mice for *K-ras*^G12D and *n* = 14 mice for *K-ras*^G12D:*Egfr*^ΔLep/ΔLep). Scale bars, 1 mm (top) and 250 μm (bottom). (**E**) Representative images of immunohistochemical staining of mouse lungs 10 weeks after tumor induction using antibodies specific for Ki67 and pERK. Tumor cell intrinsic expression of the respective proteins in at least five individual tumors per mouse was evaluated using TissueGnostics software. Graphs represent means ± SD of Ki67- and pERK-positive tumor cells normalized to all tumor cells (*n* = 5 to 7 mice per group). Scale bars, 50 μm. (**F**) Cell count of p53-deficient versus p53/EGFR double-knockout A549 cells after in vitro cultivation. Graph represents means ± SD of three individual clones per group. (**G**) Mean volumes ± SD of xenografted tumors comparing EGFR-expressing versus EGFR-deficient p53 knockout A549 cells, monitored over the course of the experiment. The graph in the middle presents the endpoint tumor weight ± SD (*n* = 6 per group). The image on the right shows the tumors at the end of the experiment. Scale bar, 2 cm. (D to G) ***P < 0.001.

isolates upon activation of the mutant *K-ras*^G12D allele in K cells (fig. S5C), as well as an overall increase in the expression of ERBB signature genes (fig. S5D). On the basis of these data, we generated a mutant K-RAS gene signature data set, which includes the 500 most up-regulated genes in K cells versus WT cells and hence depicts the most prominent alterations upon *K-ras*^G12D activation in type II pneumocytes (alveolar_

KRAS_up; table S1). Using the top 100 genes of this signature to perform unsupervised clustering analysis revealed that KE cells grouped closer to WT than to K cells, suggesting that K-RAS activity is impaired upon *Egfr* knockout (Fig. 3A). Enrichment of alveolar_KRAS_up gene signature in K cells compared to KE cells was significant (*P* < 0.001; Fig. 3B). We validated this finding by probing for additional mutant
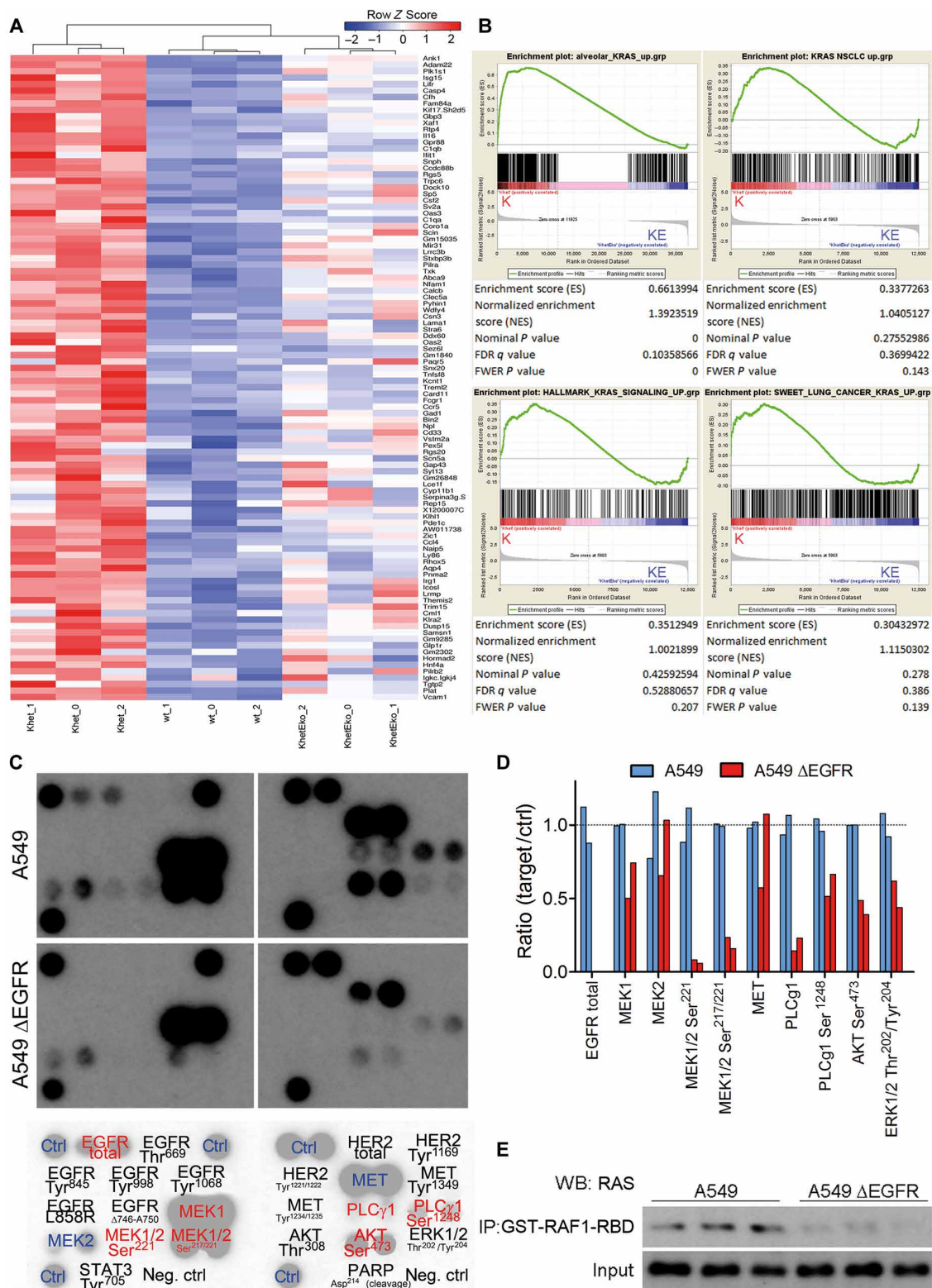
Fig. 3. Inhibition of EGFR signaling down-regulates activity of mutant K-RAS. (**A**) Heat map of top 100 up-regulated genes in *K-ras*[G12D] versus WT AT2 cells and hierarchical clustering of WT (wt_0-2), *K-ras*[G12D] (Khet_0 – 2), and *K-ras*[G12D]:*Egfr*[Δ/Δ] (KhetEko_0-2) mouse pneumocytes. (**B**) GSEA of *K-ras*[G12D] (K) versus *K-ras*[G12D]:*Egfr*[Δ/Δ] (KE) mouse pneumocytes for the indicated gene sets. (**C**) Representative image of antibody array of cell lysates of A549 and A549[ΔEGFR] cells (*n* = 2 clones per group with two spots each). Antibody probes are decoded at the bottom panel, black color indicates proteins that were not detected, red color marks proteins that were down-regulated, and blue color highlights proteins that were not differentially expressed in the A549[ΔEGFR] clones. (**D**) Densitometric quantitation of microarray films (*n* = 2 clones per group). (**E**) Western blot (WB) probing for RAS after GST-RAF1-RBD–mediated pulldown in A549 and A549[ΔEGFR] cell lysates and respective input samples (*n* = 3 per group). IP, immunoprecipitation.

Moll *et al.*, *Sci. Transl. Med.* **10**, eaao2301 (2018)   20 June 2018

5 of 12

K-RAS signature data sets (KRAS_NSCLC_up; table S2). All analyzed gene signatures were enriched in mouse alveolar K cells when compared to KE cells (Fig. 3B), indicating that deletion of EGFR suppresses K-RAS activity. *Egfr* knockout in KE also decreased ERBB signaling signatures, as evidenced by the GO ($P = 0.095$) and KEGG ($P < 0.001$) ERBB pathway gene sets, as compared to K cells (fig. S5E). Moreover, at this early time point after *K-ras*^{G12D} activation and *Egfr* knockout, the PI3K-Akt-mTOR signaling signature was decreased in KE cells, whereas EGFR-expressing K cells had an enriched signature of genes associated with poor survival of lung cancer patients (fig. S5E). In agreement with other studies (*14*, *15*), our gene expression analysis demonstrates that mutant *K-ras* activity depends on upstream EGFR expression. However, the primary cells used for RNA-seq analysis were heterozygous for the *K-ras*^{G12D} transgene, and we could not rule out an impact of the WT *K-ras* allele. Hence, we analyzed A549 cell lysates using an antibody array and found decreased phosphorylation of virtually all downstream mediators of EGFR in A549$^{\Delta EGFR}$ when compared to EGFR-expressing cells, including K-RAS downstream mediators mitogen-activated protein kinase kinases MEK1/2 and ERK1/2, suggesting a decrease in mutant K-RAS activity (Fig. 3, C and D). Using the RAS-binding domain of the RAF proto-oncogene serine/threonine-protein kinase (RAF1-RBD) for pulldown of active, guanosine 5′-triphosphate–bound RAS, we detected a reduction in activated RAS in EGFR-deficient A549 cells (Fig. 3E). To further validate inhibition of mutant K-RAS activity upon *EGFR* knockout, we took advantage of mouse KP cells and an antibody specifically recognizing mutant K-RAS^{G12D}. RAF1-RBD pulldown revealed reduced active K-RAS^{G12D} in KPE cells compared to KP cells, whereas both cell lines lacked active forms of H-RAS and N-RAS (fig. S5F). Together, these data indicate that activity of mutated K-RAS relies on activation of upstream mediators including EGFR and may represent therapeutic intervention opportunities in K-RAS–driven tumors.

Afatinib, but not erlotinib or gefitinib, reduces growth of *K-RAS*–mutated lung AC

We tested the in vitro efficacy of the EGFR TKIs afatinib, erlotinib, and gefitinib in several *K-RAS*–mutated human and mouse lung AC cell lines and included two *EGFR*-mutated cell lines as controls (fig. S6, A to C). As expected, HCC827 cells were particularly sensitive to EGFR TKI treatment because these cells harbor the *EGFR*$^{\Delta E746-A750}$ mutation. In H1975 cells, the T790M gatekeeper mutation on top of the *EGFR*^{L858R} prevented the cytotoxic effects of erlotinib and gefitinib (*29*), whereas afatinib inhibited cell growth in the nanomolar range. In *K-RAS*–mutated cell lines, afatinib exhibited an IC$_{50}$ (median inhibitory concentration) in the low micromolar range, whereas the IC$_{50}$ values of erlotinib and gefitinib were about 10- to 20-fold higher (fig. S6, A to C). When checking downstream mediators of K-RAS, we found decreased activation of ERK and MEK, as well as AKT, after short-term in vitro treatment of A549 cells with afatinib but not with erlotinib (fig. S6D). In vivo, afatinib treatment of mice reduced the growth of xenografted human cell lines A549 and A427 and of transplanted *p53*-deficient mouse 368T1 cells, which all exhibit *K-RAS* mutations (Fig. 4A). Afatinib treatment reduced the proliferation rate and induced apoptosis of grafted cells (Fig. 4, B and C). Further, we detected decreased phospho-ERK but no difference in phospho-AKT in engrafted 368T1 cells when harvested at the end of the experiment (Fig. S6, E and F).

We then evaluated patient-derived xenografts (PDXs) using tumor tissue from a *K-RAS*^{G12C}–mutated patient. The engrafted tumors were

highly sensitive to afatinib treatment, with an efficacy that was similar to that of the chemotherapeutic agent paclitaxel (Fig. 4D). However, combination therapy with afatinib and paclitaxel had no further effect on tumor volume. As in the cell line–derived xenografts, we observed reduced cell proliferation and increased apoptosis in the afatinib-treated group (Fig. 4E). We complemented these studies by using the *K-ras*^{G12D}–based GEMMs harboring autochthonous tumors. First, we treated K mice with afatinib (or vehicle control) for a period of 9 weeks, starting treatment 1 week after tumor induction. When we analyzed the lungs of these mice, we noticed reduced tumor burden in the lungs of afatinib-treated mice as compared to vehicle-treated mice (fig. S7, A and B). We also detected reduced oncogenic K-RAS^{G12D} in total lung lysates of the afatinib-treated group, which reflects the decreased amount of tumor cells in the lungs (fig. S7C). Next, we investigated whether EGFR-targeting TKIs may restrain the growth of more advanced tumors. We treated mice with already established *K-ras*^{G12D} lung AC with afatinib, erlotinib, gefitinib, or vehicle control, starting 10 weeks after tumor initiation. After another 10 weeks of treatment, mice were sacrificed and their lungs were subjected to analysis. Afatinib treatment, but not erlotinib or gefitinib, impaired the growth of *K-ras*^{G12D}–driven lung tumors. The burden in the lungs of afatinib-treated mice (20 weeks after tumor onset) was similar to lungs 10 weeks after *K-ras*^{G12D} induction (before treatment), whereas tumor areas and numbers in control and erlotinib/gefitinib-treated groups were higher (Fig. 5, A to C). These data were paralleled by a reduced lung–to–body weight ratio in the afatinib-treated group compared to the other groups, as well as by reduced *Sp-c* mRNA expression in the afatinib-treated group compared to the other groups (fig. S7, D and E). Furthermore, all afatinib-treated tumors were classified as grade I tumors, whereas most tumors in the control group were of grade II or III, as graded by board-certified pathologists (Fig. 5A) (*30*). Long-term afatinib treatment reduced tumor cell proliferation and ERK activation, but not activation of AKT (Fig. 5D and fig. S7F). Ultimately, the beneficial effects of afatinib were also highlighted in a survival analysis using the syngeneic transplant model, where 368T1 lung cancer cells were orthotopically transplanted into immunocompetent mice. Afatinib administration to these mice starting 3 weeks after transplantation significantly prolonged survival in comparison to vehicle treatment, whereas erlotinib treatment did not exhibit any beneficial effects (Fig. 5E).

Afatinib blocks a tumor escape mechanism mediated by non-EGFR ERBB family members

Puzzled by the finding that K-RAS–driven lung AC cells and tumors were sensitive to genetic *EGFR* knockout and to treatment with EGFR TKI afatinib, but not to erlotinib or gefitinib, we reanalyzed the *EGFR*-deficient A549 cell line. As stated above, we noticed that A549$^{\Delta EGFR}$ cells in early passages after gene knockout and monoclonal expansion exhibited severely reduced proliferation rates in vitro (fig. S4B). However, over time, A549$^{\Delta EGFR}$ regained their proliferative capacity, and at higher passages, there was no noticeable difference in cell growth between WT A549 and A549$^{\Delta EGFR}$ cells (fig. S8A). We performed gene expression analysis of these cells and found that in high-passage A549$^{\Delta EGFR}$ cells, the ERBB family members *ERBB2*, *ERBB3*, and *ERBB4* were up-regulated (fig. S8B), suggesting a compensatory mechanism for the loss of EGFR. Next, we checked mouse tumors in K and KE mice 20 weeks after tumor induction. The proliferation rate of KE tumors was similar to that of K tumors (Fig. 6A), indicating the activation of a compensatory program in *Egfr*-deficient tumor cells at

later time points. This was also illustrated by increased ERK phosphorylation in KE lungs versus K lungs at 20 weeks (Fig. 6B), even though both proliferation and ERK activation were down-regulated at 10 weeks (Fig. 2E). At the mRNA level, expression analysis revealed higher *ErbB2* and *ErbB4* expression in KE lungs versus K lungs compared to the 10-week time point (Fig. 6C). *ErbB3* expression was already increased at 10 weeks in KE lungs (Fig. 6C). These data were of particular interest because ERBB2 and ERBB3 were also up-regulated in human K-RAS lung AC tissue, confirming the implication of other non-EGFR ERBB family members in *K-RAS*–mutated lung tumorigenesis (Fig. 1D).

Similar to genetic knockout of *Egfr*, afatinib treatment induced up-regulation of the *ErbB* receptors in tumors of K mice (fig. S8C). To test whether this compensatory up-regulation of ERBB family members stems from the tumor cells or the stroma, we orthotopically transplanted human A549$^{\Delta p53}$ cells into NSG mice and treated the mice with afatinib or erlotinib. We noticed decreased tumor burden in lungs of afatinib-treated mice compared to erlotinib-treated mice, which was quantitated by reverse transcription polymerase chain reaction (PCR) with primers specific for A549 human housekeeping genes (Fig. 6, D and E). Further gene expression analysis revealed enhanced expression of human *EGFR*, *ERBB2*, and *ERBB3* in the tumors of afatinib-treated mice, which was comparable to up-regulation in the erlotinib-treated group (Fig. 6F). However, at the protein level, afatinib abrogated the ERBB2- and ERBB3-mediated compensatory mechanism. Afatinib markedly reduced ERBB2 protein expression and completely blocked ERBB3 activation by phosphorylation, as demonstrated in three different *K-RAS*–mutated cell lines (Fig. 6G).
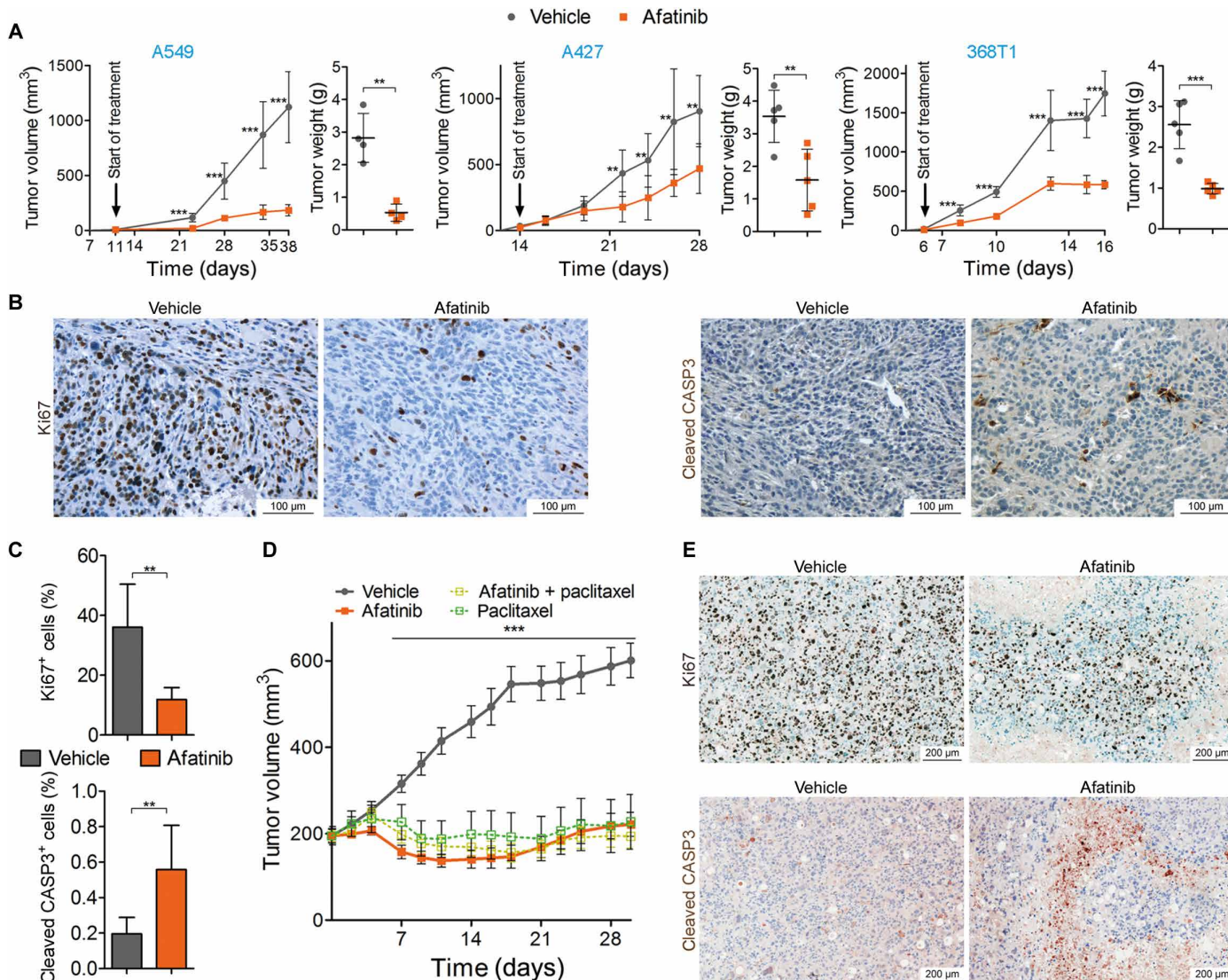

Fig. 4. Afatinib reduces growth of K-RAS–mutant lung AC in vivo. (**A**) Graphs display tumor volumes of (xeno-)grafts using indicated cell lines monitored over the experimental period and tumor weights at the end of the experiment. Mice were treated with vehicle alone or afatinib at 5 mg/kg body weight via oral gavage, five times per week, and the start of treatment is indicated. Means ± SD are shown. *n* = 4 per group in the A549 experiment and *n* ≥ 5 per group in A427 and 368T1 experiments. (**B**) Representative images of Ki67 and cleaved caspase-3 staining of 368T1 cell line–derived grafts upon vehicle and afatinib treatment. Scale bars, 100 μm. (**C**) Quantitation of positive cells in (B) (*n* = 5). (**D**) Mean tumor volumes ± SD of PDXs of lung AC tissue with *K-RAS*^{G12C} mutation. Mice were treated with vehicle, afatinib (15 mg/kg body weight, daily), paclitaxel (15 mg/kg body weight, once per week), or a combination of both treatments (*n* = 8 per group). (**E**) Representative Ki67 and cleaved caspase-3 staining for sections of vehicle-treated versus afatinib-treated PDXs. Scale bars, 200 μm. (A, C, and D) **P < 0.01, ***P < 0.001, unpaired two-tailed *t* test.

Neither erlotinib nor gefitinib had any effect on ERBB2 protein expression, and both TKIs exacerbated ERBB3 activation (ERBB4 protein expression was not detectable). Together, these data suggested that both the genetic knockout of *EGFR* and the treatment with EGFR TKIs engage a compensatory mechanism via other non-EGFR ERBB family members, which can be suppressed by afatinib but not by erlotinib or gefitinib.

Similarly, in high-passage A549$^{\Delta EGFR}$ cells, which compensated for the EGFR deficiency by increased ERBB family member expression
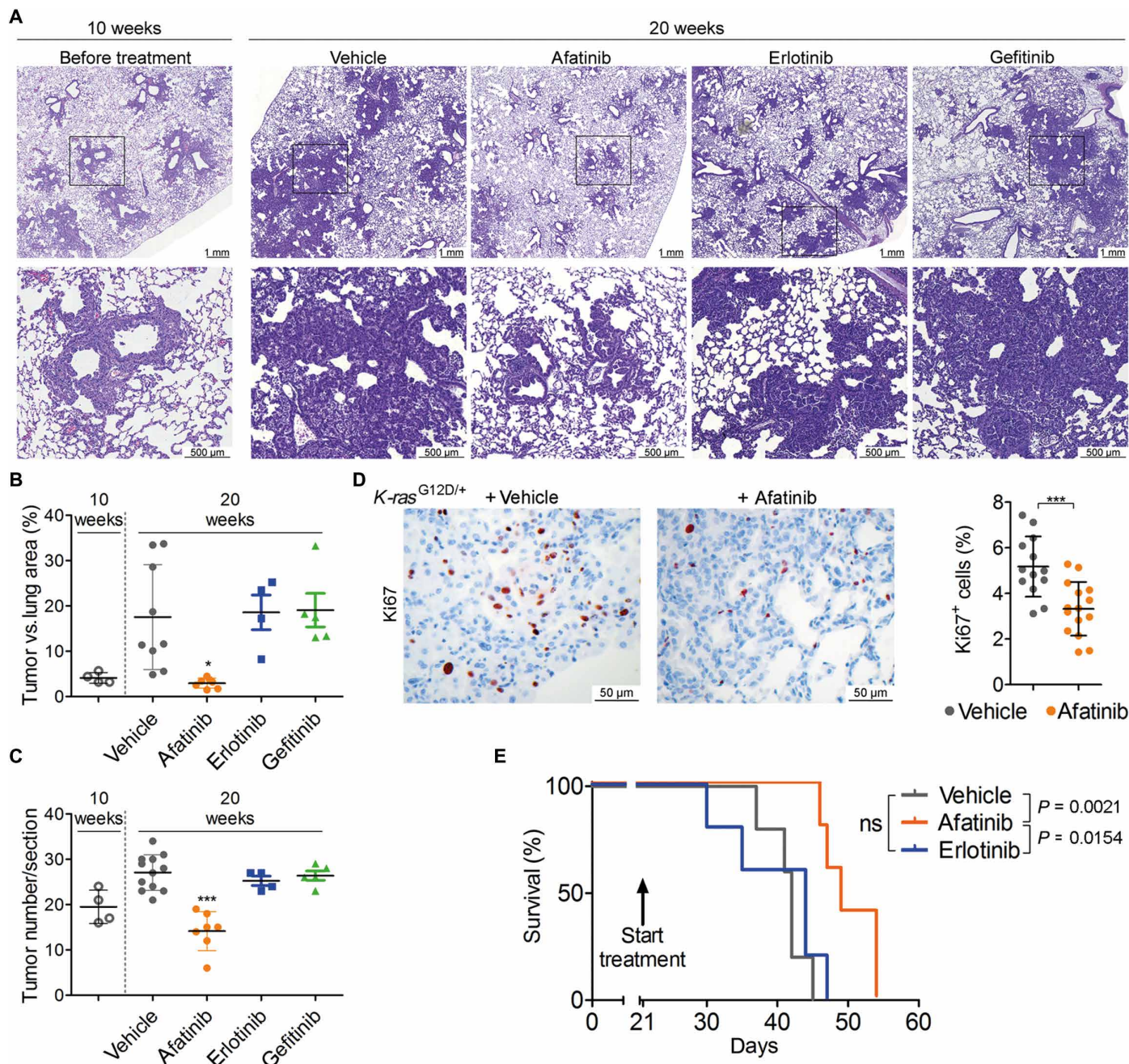
Fig. 5. Afatinib, but not first-generation EGFR TKIs, inhibits growth of autochthonous K-ras tumors. (**A**) Representative images of H&E-stained lung sections of *K-ras*$^{G12D/+}$ mice 10 weeks after Ad.Cre inhalation (left) or 20 weeks after Ad.Cre inhalation, with treatment over the last 10 weeks with vehicle, afatinib, erlotinib, or gefitinib (5 mg/kg body weight, five times per week via oral gavage). Bottom: Magnifications of the indicated sections at the top panel. $n \geq 4$ per group. Scale bars, 1 mm (top) and 500 μm (bottom). (**B** and **C**) Graphs represent means ± SD of tumor area versus total lung area ratios (B) and mean tumor numbers ± SD per section of lung (C) in mice. Each data point represents the mean value of two sections derived from one mouse. One-way analysis of variance (ANOVA) and Tukey's multiple comparison test. (**D**) Representative images of Ki67 staining of lung tumors 20 weeks after Ad.Cre induction and treated for 10 weeks with vehicle or afatinib. Ki67-positive tumor cells in at least three tumors per mouse were quantitated, and plot shows means ± SD of Ki67-positive tumor cells. Student's *t* test, $n = 4$ mice per group. Scale bars, 50 μm. (**E**) Survival analysis of immunocompetent mice after orthotopic transplantation of syngeneic 368T1 lung AC cells. Three weeks after injection, treatment with vehicle, afatinib, or erlotinib (5 mg/kg body weight, five times per week via oral gavage) was started. Median survival times were 42 days for vehicle group, 49 days for afatinib group, and 44 days for erlotinib group. Log-rank test, $n = 5$. ns, not significant. (B to E) *$P < 0.05$, ***$P < 0.001$.
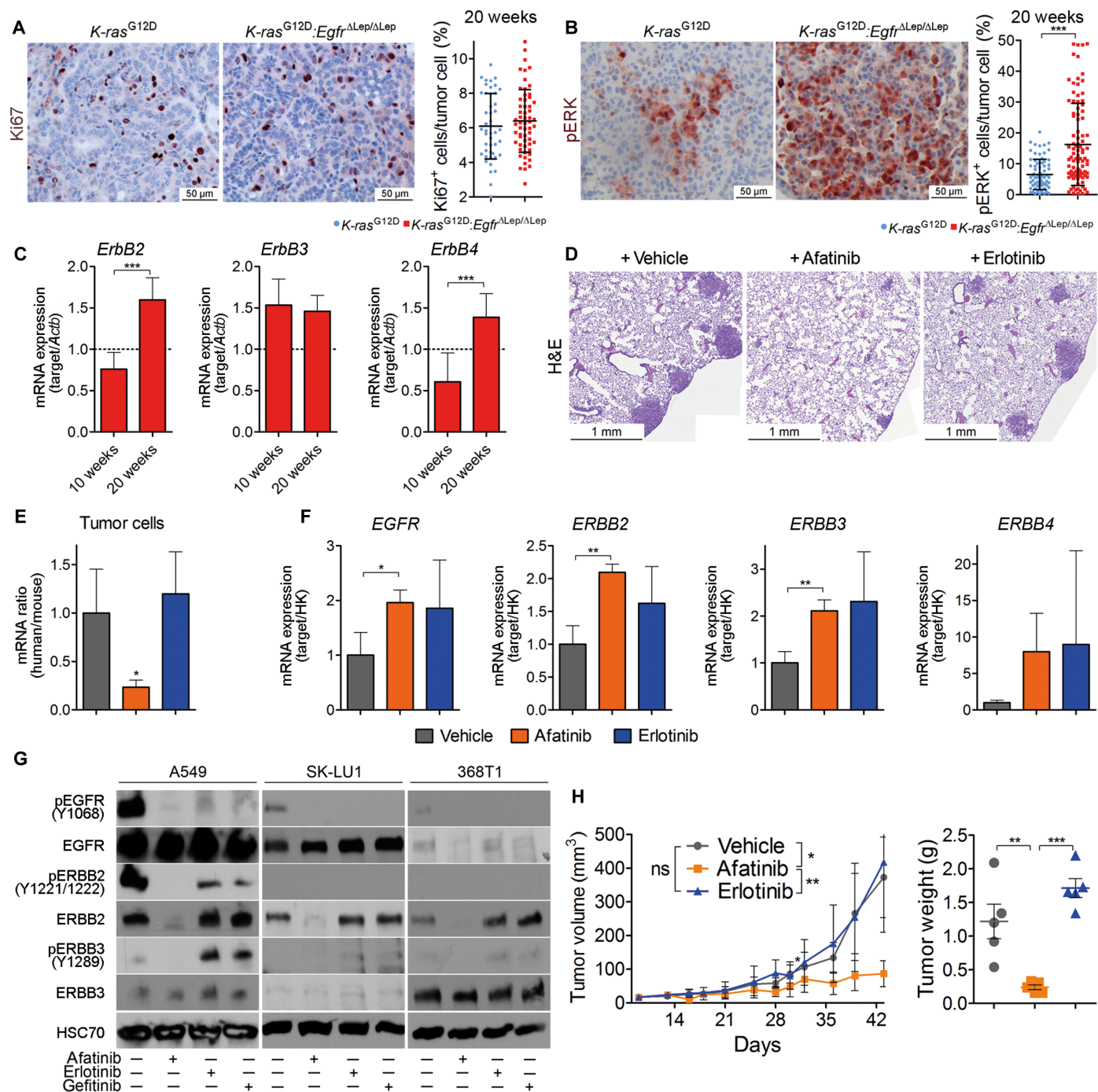
Fig. 6. ERBB family members mediate resistance to EGFR inhibition, which can be blocked by afatinib. (**A**) Representative images of Ki67 and (**B**) of pERK in lung tumors of indicated mice 20 weeks after Ad.Cre administration. The percentages of tumor cells expressing each protein were quantitated in at least eight individual tumors per mouse. Graphs represent mean percentages ± SD of Ki67- and pERK-positive tumor cells (*n* = 6 mice per group). Scale bars, 50 μm. (**C**) mRNA expression of indicated genes in lungs of *K-ras*^{G12D}:*Egfr*$^{\Delta Lep/\Delta Lep}$ mice 10 and 20 weeks after Ad.Cre inhalation. *Actb* was used as a housekeeper gene control, and relative expression of each gene was normalized to its expression in *K-ras*^{G12D} mice at the same time points (dotted line). *n* ≥ 6 per group. (**D**) Representative photographs of H&E-stained mouse lung sections, 5 weeks after orthotopic transplantation of A549$^{\Delta p53}$ cells by tail vein injection and 3 weeks after the start of treatment with vehicle, afatinib, or erlotinib (5 mg/kg body weight, five times per week via oral gavage). Scale bars, 1 mm. (**E**) Relative mRNA expression ratios of human versus mouse housekeeping genes (*ACTB* and *28S*) from mice treated as in (D). (**F**) Relative mRNA expression of human variants of the indicated genes normalized to human housekeeping genes (*ACTB* and *28S*). *n* = 3. (**G**) Western blot probing for indicated proteins in A549, SK-LU1, and 368T1 cell lysates after treatment with 1 μM afatinib, erlotinib, or gefitinib for 48 hours. (**H**) Tumor volumes of A549$^{\Delta EGFR}$ xenografts in mice receiving vehicle, afatinib, or erlotinib treatment (5 mg/kg body weight, five times per week via oral gavage), starting 14 days after transplantation, monitored over the experimental period. The graph on the right shows tumor weights at the end of the experiment. *n* ≥ 5. (A to H) **P* < 0.05, ***P* < 0.01, ****P* < 0.001.

Moll *et al.*, *Sci. Transl. Med.* **10**, eaao2301 (2018)   20 June 2018

9 of 12

and activation (fig. S8, B and D), afatinib blocked compensating ERBB2 and ERBB3 activation in vitro, but erlotinib and gefitinib did not. Finally, we xenografted high-passage A549$^{\Delta EGFR}$ cells into NSG mice and subjected them to treatment with afatinib or erlotinib. Confirming our hypothesis, afatinib treatment blocked tumor growth of EGFR-deficient/K-RAS–mutated tumor cells, whereas erlotinib did not exhibit any noticeable effect on the growth of these cells (Fig. 6H and fig. S8E). Together, these data demonstrate that both genetic and pharmacologic abrogation of EGFR-mediated signaling engages a compensatory mechanism involving other ERBB family members in K-RAS–mutated lung AC cells. Afatinib, as a pan-ERBB inhibitor, suppresses this compensatory machinery, therefore mediating a reduction of K-RAS–driven tumor growth.

DISCUSSION

Mutated K-RAS has been considered to be locked in a constitutive active state that does not require upstream signaling, and it is believed that K-RAS–driven tumors are refractory to TKI therapy (31, 32). However, recent reports using irreversible inhibitors of K-RAS^{G12C} have shown that mutated K-RAS can be hyperactivated by upstream effectors, opening the possibility of targeting receptor tyrosine kinases in K-RAS–driven tumors (14, 15). Supporting these observations, K-RAS–driven pancreatic tumors show expression of EGFR and ERBB family ligands, and they depend on EGFR and the ligand activating ADAM17 (33, 34). Similarly, we found that ERBB signaling is active in human and mouse K-RAS–driven lung AC. Advanced human tumors are enriched in an ERBB gene signature, indicating that ERBB signaling contributes to progression of K-RAS–driven AC. Supporting an active role of EGFR in tumorigenesis, genetic inactivation of EGFR impaired tumor growth in different experimental models of K-RAS–driven lung AC, irrespectively of the p53 status. In agreement with the proposed functional model of mutated K-RAS (14, 15), genetic deletion of EGFR down-regulated the activity of mutated K-RAS and downstream signaling pathways, and this may explain the observed reduction in tumorigenesis. However, over time, K-RAS–mutant tumors recovered from EGFR deletion via increased expression and activation of remaining EGFR family members, thereby restoring downstream ERK and AKT activation. This further highlights the dependence on ERBB signaling for full-blown tumorigenesis despite the oncogenic K-RAS mutation.

Most clinical studies using erlotinib and gefitinib showed little or no benefit in patients suffering from K-RAS–driven NSCLC (10–13). Similarly, erlotinib and gefitinib failed to impair tumorigenesis in all our experimental models of K-RAS–driven AC, although tumors transiently responded to genetic deletion of EGFR. This may be attributed to the inherent differences between the genetic and pharmacological approaches. EGFR mediates kinase-independent functions in cancer cell survival (35, 36), and whereas total EGFR knockout mice are not viable, animals with severely suppressed EGFR kinase activity display only minor epithelial defects (37–39). However, in our study, both genetic EGFR deletion and erlotinib treatment triggered a similar tumor escape mechanism, relying on the activation of non-EGFR ERBB family members, although the initiation of this mechanism was delayed upon EGFR knockout compared to TKI-mediated inhibition. This rapid response to TKI treatment may be responsible for the failure of the first-generation TKIs in K-RAS–driven NSCLC. Afatinib abrogated the activation of ERBB family members, suppressed the tumor compensatory mechanism, and resulted in an efficient inhibition of K-RAS–driven lung AC. Similarly, pan-ERBB inhibition with a mixture of monoclonal antibodies (pan-HER) suppresses tumorigenesis more efficiently than targeting single ERBB receptors (40). Notably, we and Kruspig et al. (41) found that irreversible TKIs such as afatinib or neratinib down-regulate ERBB2 and ERBB3 proteins, a similar phenomenon to that observed with pan-HER antibodies (40), which may contribute to the efficacy of irreversible TKIs.

A limitation of our study is the use of preclinical experimental models that may not faithfully recapitulate their human counterparts. In this sense, our mouse models do not resemble human mucinous lung AC because of the differences in NKX2-1 expression (42). In addition, human tumor complexity and heterogeneity are not properly modeled in mouse lung AC. Despite these experimental limitations, our data suggest that, in contrast to current opinion, resistance to first-generation TKIs in K-RAS–driven NSCLC may not be due to constitutive activation of K-RAS but rather due to a (re)activation of other ERBB family members. These findings suggest that pan-ERBB inhibitors such as afatinib, alone or in combination with other inhibitors, including MEK (41, 43) or K-RAS^{G12C} inhibitors, are potent therapeutic agents for treatment of patients with K-RAS–mutated NSCLC.

MATERIALS AND METHODS

Study design

The goal of the study was to revisit the role of EGFR-mediated signaling in K-RAS–driven lung tumorigenesis. Hence, we used publicly available data sets, biopsies of patients, in vitro model systems, and mouse models for analysis. To calculate the minimal mouse number (sample size) for Kaplan-Meier analysis, we used a Web-based tool (www.cct. cuhk.edu.hk/stat/survival/Rubinstein1981.htm) and the following parameters: $\alpha = 0.0125$; $\beta = 0.05$; $\delta = 0.12$, Ms = 5.75 months; proportion of control group (QC) = 0.5; proportion of experiment group (QE) = 0.5; T0 = 2 months; T-T0 = 8 months. For the time point analysis (10 and 20 weeks after tumor initiation), we used the Web tool (www. quantitativeskills.com/sisa/calculations/samsize.htm) and the following parameters: Mean 1 (Exp.): 10.90/21.33; mean 2 (Obs.): 6.105/6.333; SD1: 2.937/12.01; SD2: 3.037/4.041; allocation ratio = 1; power = 95; alpha = 5. In the course of the experiments, calculated sample numbers were adjusted according to the availability of the respective mice. For our in vivo studies using TKIs, we randomly assigned mice to the different treatment groups before the start of the experiment, for example, to rAd.Cre inhalation or tumor cell injection. Tissue was harvested and processed in a random and blinded order. All other experiments were performed with several biological replicates (as indicated in figure legends), and all replicates were included in our data analysis. As a common guideline in our laboratory, we determined outliers and excluded them from analysis according to the following rule: If a number is less than Q1 − 1.5 × IQR or greater than Q3 + 1.5 × IQR, then it is considered to be an outlier, with IQR being the interquartile range, equal to the difference between the third quartile (Q3) and first quartile (Q1). All outliers are marked in red color in table S3.

Statistical analysis

GraphPad Prism 5.0 was used for statistical analysis. All values are given as means ± SD, as indicated in figure legends. Comparisons between two groups were made by Student's t test, except for Kaplan-Meier analysis, where we used a log-rank test. For comparison of more than two groups, we used ANOVA with subsequent Tukey's multiple comparison test. We did not use any statistical method to predetermine sample size in animal studies.

Moll et al., Sci. Transl. Med. 10, eaao2301 (2018)   20 June 2018

10 of 12

SUPPLEMENTARY MATERIALS

www.sciencetranslationalmedicine.org/cgi/content/full/10/446/eaao2301/DC1

Materials and Methods

Fig. S1. *K-RAS*–mutated lung ACs display increased ERBB expression profile.

Fig. S2. *K-RAS*–mutated lung ACs exhibit activated EGFR.

Fig. S3. Genetic EGFR ablation in *K-RAS*–mutated lung AC reduces tumor growth.

Fig. S4. Genetic EGFR ablation in *K-RAS*–mutated lung AC cells reduces tumor growth.

Fig. S5. Inhibition of EGFR signaling down-regulates mutated K-RAS activity.

Fig. S6. Afatinib reduces growth of K-RAS–mutant lung AC in vitro.

Fig. S7. Afatinib reduces K-RAS–mediated tumorigenesis in vivo.

Fig. S8. ERBB family members mediate resistance to EGFR inhibition, which can be blocked by afatinib.

Table S1. Alveolar_KRAS_up gene set (provided as an Excel file).

Table S2. KRAS_NSCLC_up gene set (provided as an Excel file).

Table S3. Primary data shown in the figures (provided as an Excel file).

Table S4. List of genotyping primers.

Table S5. List of primers for quantitative PCR analysis.

References (*44–51*)

REFERENCES AND NOTES

1. R. L. Siegel, K. D. Miller, A. Jemal, Cancer statistics, 2016. *CA Cancer J. Clin.* **66**, 7–30 (2016).

2. Cancer Genome Atlas Research Network, Comprehensive molecular profiling of lung adenocarcinoma. *Nature* **511**, 543–550 (2014).

3. C. Swanton, R. Govindan, Clinical implications of genomic discoveries in lung cancer. *N. Engl. J. Med.* **374**, 1864–1873 (2016).

4. S. Kobayashi, T. J. Boggon, T. Dayaram, P. A. Jänne, O. Kocher, M. Meyerson, B. E. Johnson, M. J. Eck, D. G. Tenen, B. Halmos, EGFR mutation and resistance of non-small-cell lung cancer to gefitinib. *N. Engl. J. Med.* **352**, 786–792 (2005).

5. W. Pao, V. Miller, M. Zakowski, J. Doherty, K. Politi, I. Sarkaria, B. Singh, R. Heelan, V. Rusch, L. Fulton, E. Mardis, D. Kupfer, R. Wilson, M. Kris, H. Varmus, EGF receptor gene mutations are common in lung cancers from "never smokers" and are associated with sensitivity of tumors to gefitinib and erlotinib. *Proc. Natl. Acad. Sci. U.S.A.* **101**, 13306–13311 (2004).

6. C. H. Yun, K. E. Mengwasser, A. V. Toms, M. S. Woo, H. Greulich, K. K. Wong, M. Meyerson, M. J. Eck, The T790M mutation in EGFR kinase causes drug resistance by increasing the affinity for ATP. *Proc. Natl. Acad. Sci. U.S.A.* **105**, 2070–2075 (2008).

7. Y. L. Wu, C. Zhou, C. P. Hu, J. Feng, S. Lu, Y. Huang, W. Li, M. Hou, J. H. Shi, K. Y. Lee, C. R. Xu, D. Massey, M. Kim, Y. Shi, S. L. Geater, Afatinib versus cisplatin plus gemcitabine for first-line treatment of Asian patients with advanced non-small-cell lung cancer harbouring EGFR mutations (LUX-Lung 6): An open-label, randomised phase 3 trial. *Lancet Oncol.* **15**, 213–222 (2014).

8. A. D. Cox, S. W. Fesik, A. C. Kimmelman, J. Luo, C. J. Der, Drugging the undruggable RAS: Mission possible? *Nat. Rev. Drug Discov.* **13**, 828–851 (2014).

9. S. Gysin, M. Salt, A. Young, F. McCormick, Therapeutic strategies for targeting ras proteins. *Genes Cancer* **2**, 359–372 (2011).

10. H. Linardou, I. J. Dahabreh, D. Kanaloupiti, F. Siannis, D. Bafaloukos, P. Kosmidis, C. A. Papadimitriou, S. Murray, Assessment of somatic k-RAS mutations as a mechanism associated with resistance to EGFR-targeted agents: A systematic review and meta-analysis of studies in advanced non-small-cell lung cancer and metastatic colorectal cancer. *Lancet Oncol.* **9**, 962–972 (2008).

11. C. Mao, L. X. Qiu, R. Y. Liao, F. B. Du, H. Ding, W. C. Yang, J. Li, Q. Chen, KRAS mutations and resistance to EGFR-TKIs treatment in patients with non-small cell lung cancer: A meta-analysis of 22 studies. *Lung Cancer* **69**, 272–278 (2010).

12. E. Rulli, M. Marabese, V. Torri, G. Farina, S. Veronese, A. Bettini, F. Longo, L. Moscetti, M. Ganzinelli, C. Lauricella, E. Copreni, R. Labianca, O. Martelli, S. Marsoni, M. Broggini, M. C. Garassino; TAILOR Trialists, Value of KRAS as prognostic or predictive marker in NSCLC: Results from the TAILOR trial. *Ann. Oncol.* **26**, 2079–2084 (2015).

13. V. Papadimitrakopoulou, J. J. Lee, I. I. Wistuba, A. S. Tsao, F. V. Fossella, N. Kalhor, S. Gupta, L. A. Byers, J. G. Izzo, S. N. Gettinger, S. B. Goldberg, X. Tang, V. A. Miller, F. Skoulidis, D. L. Gibbons, L. Shen, C. Wei, L. Diao, S. A. Peng, J. Wang, A. L. Tam, K. R. Coombes, J. S. Koo, D. J. Mauro, E. H. Rubin, J. V. Heymach, W. K. Hong, R. S. Herbst, The BATTLE-2 Study: A biomarker-integrated targeted therapy study in previously treated patients with advanced non-small-cell lung cancer. *J. Clin. Oncol.* **1**, JCO660084 (2016).

14. P. Lito, M. Solomon, L. S. Li, R. Hansen, N. Rosen, Allele-specific inhibitors inactivate mutant KRAS G12C by a trapping mechanism. *Science* **351**, 604–608 (2016).

15. M. P. Patricelli, M. R. Janes, L. S. Li, R. Hansen, U. Peters, L. V. Kessler, Y. Chen, J. M. Kucharski, J. Feng, T. Ely, J. H. Chen, S. J. Firdaus, A. Babbar, P. Ren, Y. Liu, Selective inhibition of oncogenic KRAS output with small molecules targeting the inactive state. *Cancer Discov.* **6**, 316–329 (2016).

16. L. Girard, J. Rodriguez-Canales, C. Behrens, D. M. Thompson, I. W. Botros, H. Tang, Y. Xie, N. Rekhtman, W. D. Travis, I. I. Wistuba, J. D. Minna, A. F. Gazdar, An expression signature as an aid to the histologic classification of non-small cell lung cancer. *Clin. Cancer Res.* **22**, 4880–4889 (2016).

17. A. Subramanian, P. Tamayo, V. K. Mootha, S. Mukherjee, B. L. Ebert, M. A. Gillette, A. Paulovich, S. L. Pomeroy, T. R. Golub, E. S. Lander, J. P. Mesirov, Gene set enrichment analysis: A knowledge-based approach for interpreting genome-wide expression profiles. *Proc. Natl. Acad. Sci. U.S.A.* **102**, 15545–15550 (2005).

18. W. Han, T. Zhang, H. Yu, J. G. Foulke, C. K. Tang, Hypophosphorylation of residue Y1045 leads to defective downregulation of EGFRvIII. *Cancer Biol. Ther.* **5**, 1361–1368 (2006).

19. E. L. Jackson, N. Willis, K. Mercer, R. T. Bronson, D. Crowley, R. Montoya, T. Jacks, D. A. Tuveson, Analysis of lung tumor initiation and progression using conditional expression of oncogenic *K-ras*. *Genes Dev.* **15**, 3243–3248 (2001).

20. B. Grabner, D. Schramek, K. M. Mueller, H. P. Moll, J. Svinka, T. Hoffmann, E. Bauer, L. Blaas, N. Hruschka, K. Zboray, P. Stiedl, H. Nivarthi, E. Bogner, W. Gruber, T. Mohr, R. H. Zwick, L. Kenner, V. Poli, F. Aberger, D. Stoiber, G. Egger, H. Esterbauer, J. Zuber, R. Moriggl, R. Eferl, B. Győrffy, J. M. Penninger, H. Popper, E. Casanova, Disruption of STAT3 signalling promotes KRAS-induced lung tumorigenesis. *Nat. Commun.* **6**, 6285 (2015).

21. A. Natarajan, B. Wagner, M. Sibilia, The EGF receptor is required for efficient liver regeneration. *Proc. Natl. Acad. Sci. U.S.A.* **104**, 17081–17086 (2007).

22. J. Jonkers, R. Meuwissen, H. van der Gulden, H. Peterse, M. van der Valk, A. Berns, Synergistic tumor suppressor activity of BRCA2 and p53 in a conditional mouse model for breast cancer. *Nat. Genet.* **29**, 418–425 (2001).

23. E. L. Jackson, K. P. Olive, D. A. Tuveson, R. Bronson, D. Crowley, M. Brown, T. Jacks, The differential effects of mutant p53 alleles on advanced murine lung cancer. *Cancer Res.* **65**, 10280–10288 (2005).

24. H. Choi, J. Sheng, D. Gao, F. Li, A. Durrans, S. Ryu, S. B. Lee, N. Narula, S. Rafii, O. Elemento, N. K. Altorki, S. T. Wong, V. Mittal, Transcriptome analysis of individual stromal cell populations identifies stroma-tumor crosstalk in mouse lung cancer model. *Cell Rep.* **10**, 1187–1201 (2015).

25. T. Kamata, S. Giblett, C. Pritchard, KRAS^G12D expression in lung-resident myeloid cells promotes pulmonary LCH-like neoplasm sensitive to statin treatment. *Blood* **130**, 514–526 (2017).

26. X. Xu, J. R. Rock, Y. Lu, C. Futtner, B. Schwab, J. Guinney, B. L. Hogan, M. W. Onaitis, Evidence for type II cells as cells of origin of K-Ras-induced distal lung adenocarcinoma. *Proc. Natl. Acad. Sci. U.S.A.* **109**, 4910–4915 (2012).

27. T. J. Desai, D. G. Brownfield, M. A. Krasnow, Alveolar progenitor and stem cells in lung development, renewal and cancer. *Nature* **507**, 190–194 (2014).

28. S. Mainardi, N. Mijimolle, S. Francoz, C. Vicente-Dueñas, I. Sánchez-García, M. Barbacid, Identification of cancer initiating cells in *K-Ras* driven lung adenocarcinoma. *Proc. Natl. Acad. Sci. U.S.A.* **111**, 255–260 (2014).

29. W. Pao, V. A. Miller, K. A. Politi, G. J. Riely, R. Somwar, M. F. Zakowski, M. G. Kris, H. Varmus, Acquired resistance of lung adenocarcinomas to gefitinib or erlotinib is associated with a second mutation in the EGFR kinase domain. *PLOS Med.* **2**, e73 (2005).

30. M. DuPage, A. L. Dooley, T. Jacks, Conditional mouse lung cancer models using adenoviral or lentiviral delivery of Cre recombinase. *Nat. Protoc.* **4**, 1064–1072 (2009).

31. W. Pao, T. Y. Wang, G. J. Riely, V. A. Miller, Q. Pan, M. Ladanyi, M. F. Zakowski, R. T. Heelan, M. G. Kris, H. E. Varmus, *KRAS* mutations and primary resistance of lung adenocarcinomas to gefitinib or erlotinib. *PLOS Med.* **2**, e17 (2005).

32. W. Brugger, N. Triller, M. Blasinska-Morawiec, S. Curescu, R. Sakalauskas, G. M. Manikhas, J. Mazieres, R. Whittom, C. Ward, K. Mayne, K. Trunzer, F. Cappuzzo, Prospective molecular marker analyses of EGFR and KRAS from a randomized, placebo-controlled study of erlotinib maintenance therapy in advanced non-small-cell lung cancer. *J. Clin. Oncol.* **29**, 4113–4120 (2011).

33. C. M. Ardito, B. M. Grüner, K. K. Takeuchi, C. Lubeseder-Martellato, N. Teichmann, P. K. Mazur, K. E. Delgiorno, E. S. Carpenter, C. J. Halbrook, J. C. Hall, D. Pal, T. Briel, A. Herner, M. Trajkovic-Arsic, B. Sipos, G. Y. Liou, P. Storz, N. R. Murray, D. W. Threadgill, M. Sibilia, M. K. Washington, C. L. Wilson, R. M. Schmid, E. W. Raines, H. C. Crawford, J. T. Siveke, EGF receptor is required for KRAS-induced pancreatic tumorigenesis. *Cancer Cell* **22**, 304–317 (2012).

34. C. Navas, I. Hernández-Porras, A. J. Schuhmacher, M. Sibilia, C. Guerra, M. Barbacid, EGF receptor signaling is essential for k-ras oncogene-driven pancreatic ductal adenocarcinoma. *Cancer Cell* **22**, 318–330 (2012).

35. J. A. Ewald, J. C. Wilkinson, C. A. Guyer, J. V. Staros, Ligand- and kinase activity-independent cell survival mediated by the epidermal growth factor receptor expressed in 32D cells. *Exp. Cell Res.* **282**, 121–131 (2003).

36. Z. Weihua, R. Tsan, W. C. Huang, Q. Wu, C. H. Chiu, I. J. Fidler, M. C. Hung, Survival of cancer cells is maintained by EGFR independent of its kinase activity. *Cancer Cell* **13**, 385–393 (2008).

37. P. J. Miettinen, J. E. Berger, J. Meneses, Y. Phung, R. A. Pedersen, Z. Werb, R. Derynck, Epithelial immaturity and multiorgan failure in mice lacking epidermal growth factor receptor. *Nature* **376**, 337–341 (1995).

Moll *et al.*, *Sci. Transl. Med.* **10**, eaao2301 (2018) 20 June 2018

11 of 12

38. N. C. Luetteke, H. K. Phillips, T. H. Qiu, N. G. Copeland, H. S. Earp, N. A. Jenkins, D. C. Lee, The mouse waved-2 phenotype results from a point mutation in the EGF receptor tyrosine kinase. *Genes Dev.* **8**, 399–413 (1994).

39. M. Sibilia, E. F. Wagner, Strain-dependent epithelial defects in mice lacking the EGF receptor. *Science* **269**, 234–238 (1995).

40. H. J. Jacobsen, T. T. Poulsen, A. Dahlman, I. Kjaer, K. Koefoed, J. W. Sen, D. Weilguny, B. Bjerregaard, C. R. Andersen, I. D. Horak, M. W. Pedersen, M. Kragh, J. Lantto, Pan-HER, an antibody mixture simultaneously targeting EGFR, HER2, and HER3, effectively overcomes tumor heterogeneity and plasticity. *Clin. Cancer Res.* **21**, 4110–4122 (2015).

41. B. Kruspig, T. Monteverde, S. Neidler, A. Hock, E. Kerr, C. Nixon, W. Clark, A. Hedley, S. Laing, S. B. Coffelt, J. Le Quesne, C. Dick, K. Vousden, C. P. Martins, D. J. Murphy, The ERBB network facilitates KRAS-driven lung tumorigenesis. *Sci. Transl. Med.* **10**, eaao2565 (2018).

42. R. Kunii, S. Jiang, G. Hasegawa, T. Yamamoto, H. Umezu, T. Watanabe, M. Tsuchida, T. Hashimoto, T. Hamakubo, T. Kodama, K. Sasai, M. Naito, The predominant expression of hepatocyte nuclear factor 4α (HNF4α) in thyroid transcription factor-1 (TTF-1)-negative pulmonary adenocarcinoma. *Histopathology* **58**, 467–476 (2011).

43. C. Sun, S. Hobor, A. Bertotti, D. Zecchin, S. Huang, F. Galimi, F. Cottino, A. Prahallad, W. Grernrum, A. Tzani, A. Schlicker, L. F. Wessels, E. F. Smit, E. Thunnissen, P. Halonen, C. Lieftink, R. L. Beijersbergen, F. Di Nicolantonio, A. Bardelli, L. Trusolino, R. Bernards, Intrinsic resistance to MEK inhibition in KRAS mutant lung and colon cancer through transcriptional induction of ERBB3. *Cell Rep.* **7**, 86–93 (2014).

44. V. K. Mootha, C. M. Lindgren, K.-F. Eriksson, A. Subramanian, S. Sihag, J. Lehar, P. Puigserver, E. Carlsson, M. Ridderstråle, E. Laurila, N. Houstis, M. J. Daly, N. Patterson, J. P. Mesirov, T. R. Golub, P. Tamayo, B. Spiegelman, E. S. Lander, J. N. Hirschhorn, D. Altshuler, L. C. Groop, PGC-1α-responsive genes involved in oxidative phosphorylation are coordinately downregulated in human diabetes. *Nat. Genet.* **34**, 267–273 (2003).

45. S. Babicki, D. Arndt, A. Marcu, Y. Liang, J. R. Grant, A. Maciejewski, D. S. Wishart, Heatmapper: Web-enabled heat mapping for all. *Nucleic Acids Res.* **44**, W147–W153 (2016).

46. M. M. Winslow, T. L. Dayton, R. G. W. Verhaak, C. Kim-Kiselak, E. L. Snyder, D. M. Feldser, D. D. Hubbard, M. J. DuPage, C. A. Whittaker, S. Hoersch, S. Yoon, D. Crowley, R. T. Bronson, D. Y. Chiang, M. Meyerson, T. Jacks, Suppression of lung adenocarcinoma progression by Nkx2-1. *Nature* **473**, 101–104 (2011).

47. D. M. Euhus, C. Hudd, M. C. LaRegina, F. E. Johnson, Tumor measurement in the nude mouse. *J. Surg. Oncol.* **31**, 229–234 (1986).

48. F. A. Ran, P. D. Hsu, J. Wright, V. Agarwala, D. A. Scott, F. Zhang, Genome engineering using the CRISPR-Cas9 system. *Nat. Protoc.* **8**, 2281–2308 (2013).

49. E. K. Brinkman, T. Chen, M. Amendola, B. van Steensel, Easy quantitative assessment of genome editing by sequence trace decomposition. *Nucleic Acids Res.* **42**, e168 (2014).

50. M. W. Pfaffl, A new mathematical model for relative quantification in real-time RT-PCR. *Nucleic Acids Res.* **29**, e45 (2001).

51. M. W. Pfaffl, A. Tichopad, C. Prgomet, T. P. Neuvians, Determination of stable housekeeping genes, differentially regulated target genes and sample integrity: BestKeeper–excel-based tool using pair-wise correlations. *Biotechnol. Lett.* **26**, 509–515 (2004).

Citation: H. P. Moll, K. Pranz, M. Musteanu, B. Grabner, N. Hruschka, J. Mohrherr, P. Aigner, P. Stiedl, L. Brcic, V. Laszlo, D. Schramek, R. Moriggl, R. Eferl, J. Moldvay, K. Dezso, P. P. Lopez-Casas, D. Stoiber, M. Hidalgo, J. Penninger, M. Sibilia, B. Győrffy, M. Barbacid, B. Dome, H. Popper, E. Casanova, Afatinib restrains K-RAS–driven lung tumorigenesis. *Sci. Transl. Med.* **10**, eaao2301 (2018).

Moll *et al.*, *Sci. Transl. Med.* **10**, eaao2301 (2018)   20 June 2018

12 of 12

Science Translational Medicine

Afatinib restrains K-RAS–driven lung tumorigenesis

Herwig P. Moll, Klemens Pranz, Monica Musteanu, Beatrice Grabner, Natascha Hruschka, Julian Mohrherr, Petra Aigner, Patricia Stiedl, Luka Brcic, Viktoria Laszlo, Daniel Schramek, Richard Moriggl, Robert Eferl, Judit Moldvay, Katalin Dezso, Pedro P. Lopez-Casas, Dagmar Stoiber, Manuel Hidalgo, Josef Penninger, Maria Sibilia, Balázs Gyorffy, Mariano Barbacid, Balázs Dome, Helmut Popper and Emilio Casanova

A new role for kinase inhibitors

The K-RAS oncogene is frequently mutated in a variety of cancer types, including lung cancer. Lung cancers with K-RAS mutations are usually difficult to target, and conventional thinking dictates that these tumors are resistant to receptor tyrosine kinase inhibitors because those act upstream of the constitutively active K-RAS protein. However, it appears that receptor tyrosine kinase signaling may have an effect on K-RAS–driven lung tumors after all, by amplifying their growth beyond the effects of K-RAS alone. Kruspig *et al.* and Moll *et al.* independently reached this conclusion and identified approved multikinase inhibitors that are effective in the setting of K-RAS–mutant lung cancer in multiple mouse models, suggesting that this may be a potential treatment strategy for human patients as well.

ARTICLE TOOLS	http://stm.sciencemag.org/content/10/446/eaao2301
SUPPLEMENTARY MATERIALS	http://stm.sciencemag.org/content/suppl/2018/06/18/10.446.eaao2301.DC1
RELATED CONTENT	http://stm.sciencemag.org/content/scitransmed/10/446/eaao2565.full http://stm.sciencemag.org/content/scitransmed/10/431/eaan8840.full http://stm.sciencemag.org/content/scitransmed/9/416/eaan6566.full http://stm.sciencemag.org/content/scitransmed/9/394/eaal5253.full
REFERENCES	This article cites 51 articles, 17 of which you can access for free http://stm.sciencemag.org/content/10/446/eaao2301#BIBL
PERMISSIONS	http://www.sciencemag.org/help/reprints-and-permissions

Use of this article is subject to the Terms of Service